

Single-particle view of stress-promoters induction dynamics: an interplay between MAPK signaling, chromatin and transcription factors

Victoria Wosika and Serge Pelet*

Department of Fundamental Microbiology

University of Lausanne

1015 Lausanne, Switzerland.

*Correspondance : serge.pelet@unil.ch

Abstract

Precise regulation of gene expression in response to environmental changes is crucial for cell survival, adaptation and proliferation. In eukaryotic cells, extracellular signal integration is often carried out by Mitogen-Activated Protein Kinases (MAPK). Despite a robust MAPK signaling activity, downstream gene expression can display a great variability between single cells. Using a live mRNA reporter, we monitored the dynamics of transcription in *Saccharomyces cerevisiae* upon hyper-osmotic shock. The transient activity of the MAPK Hog1 opens a temporal window where stress-response genes can be activated. Here we show that the first minutes of Hog1 activity are essential to control the activation of a promoter. The chromatin repression on a locus slows down this transition and contributes to the variability in gene expression, while binding of transcription factors increases the level of transcription. However, soon after Hog1 activity peaks, negative regulators promote chromatin closure of the locus and transcription progressively stops.

1 Introduction

2 A crucial function of all cellular life is the ability to sense its surroundings and adapt to
3 its variations. These changes in the extracellular environment will induce specific
4 cellular responses, orchestrated by signal transduction cascades which receive cues
5 from plasma membrane sensors. This information is turned into a biological response
6 by inducing complex transcriptional programs implicating hundreds of genes¹⁻³. Tight
7 regulation of signaling is thus crucial to ensure the correct temporal modulation of gene
8 expression, which can otherwise alter the cell physiology⁴⁻⁶. Interestingly, single-cell
9 analyses have revealed that genes regulated by an identical signaling activity can
10 display a high variability in their transcriptional responses⁷⁻¹⁰. This noise in
11 transcriptional output questions how signal transduction can faithfully induce different
12 loci and which molecular mechanisms contribute to the variability in gene expression.

13 In eukaryotic cells, various environmental stimuli are transduced by the highly
14 conserved Mitogen-Activated Protein Kinases (MAPK) cascades^{11,12}. They control a
15 wide range of cellular responses from cell proliferation, differentiation or apoptosis. In
16 *Saccharomyces cerevisiae*, a sudden increase in the osmolarity of the medium is
17 sensed by the High Osmolarity Glycerol (HOG) pathway, which leads to the activation
18 of the MAPK Hog1, a homolog of p38 in mammals^{13,14}. Upon hyper-osmotic stress, the
19 kinase activity of Hog1 promotes the adaptation of the cells to their new environment
20 by driving an increase in the internal glycerol concentration, thereby allowing to
21 balance the internal and the external osmotic pressures. In parallel to its cytoplasmic
22 activity, Hog1 also transiently accumulates into the nucleus to induce the expression
23 of hundreds of osmostress-responsive genes (Fig. 1a). The MAPK is recruited to
24 promoter regions by Transcription Factors (TFs) and, in turn, Hog1 recruits chromatin
25 remodeling complexes, the Pre-Initiation Complex and the RNA Polymerase II (PolII)
26 to trigger gene expression^{15,16}. Once cells have adapted, Hog1 is inactivated and exits
27 the cell nucleus, transcription stops and chromatin is rapidly reassembled at HOG-
28 induced gene loci.

29 Biochemical analyses of this pathway have identified the key players implicated in
30 gene expression and the central role played by the MAPK in all these steps¹⁵. In

31 parallel, single-cell measurements have uncovered the large variability present in their
32 expression. In particular, translational reporters and RNA-FISH measurements have
33 identified that slow chromatin remodeling promoted by the MAPK at each individual
34 locus is generating strong intrinsic noise in the activation of many stress-responsive
35 genes^{9,17}.

36 In order to get deeper insights into the regulation of osmostress-genes expression
37 kinetics, we aimed at monitoring the dynamics of mRNA production in live single cells.
38 Phage coat protein-based assays, like the MS2 or PP7 systems, have been used to
39 visualize mRNA in live single cells^{18–20}. These experiments contributed to revealing the
40 bursty nature of transcription, whereby a set of polymerases simultaneously
41 transcribing a gene generates a burst in mRNA production, which is followed by a
42 pause in transcription^{21–23}.

43 In this study, we dissect the kinetics of transcription of osmostress-genes. The
44 production of mRNA is monitored using the PP7 phage coat protein assay. This
45 reporter allows us to measure with high temporal resolution and in a fully automated
46 manner, the fluctuations in transcription arising in hundreds of live single cells. This
47 analysis enables to dissect the contribution of various players to the overall
48 transcriptional output. We show that the first few minutes of MAPK activity will
49 determine if a gene is transcribed. We also demonstrate that the chromatin state of a
50 promoter will control the timing of activation and thus the variability of the transcription,
51 while the TF binding will influence the level and duration of the mRNA production.

52 **Results**

53 High osmotic pressure is sensed and transduced in the budding yeast *Saccharomyces*
54 *cerevisiae* via the HOG signaling cascade, which culminates in the activation of the
55 MAPK Hog1 (Fig. 1a). Upon activation, this key regulator accumulates in the nucleus
56 to trigger gene expression in a stress level-dependent manner (Supplementary Figure
57 1a). The activity of the kinase can be monitored by following its own nuclear
58 enrichment^{24,25}. In parallel to Hog1, the general stress response pathway is induced
59 by the hyper-osmotic shock and the transcription factor Msn2 also relocate into the
60 nucleus with dynamics highly similar to the ones observed for Hog1 (Supplementary

61 Figure 1b and c)^{26,27}. Nuclear Hog1 and Msn2 (together with its paralog Msn4) induce
62 osmostress-genes expression, with approximately 250 genes being up-regulated upon
63 osmotic shock^{1,28,29}. The activity of the pathway is limited to the cellular adaptation
64 time, which coincide with the nuclear exit of Hog1 and the recovery of the cell size
65 (Supplementary Figure 1a and d). The fast and transient activity of the osmostress
66 response as well as the homogenous activation of the MAPK within the population^{9,25}
67 (Supplementary Figure 1e), make this signaling pathway an excellent model to
68 understand the induction of eukaryotic stress-responsive genes, which are often
69 accompanied by important chromatin remodeling.

70 *Monitoring the dynamics of osmostress-genes transcription*

71 In order to quantify the dynamics of transcription in live single cells, we use the PP7
72 system to label the production of messenger RNAs (mRNA)³⁰. Briefly, constitutively
73 expressed and fluorescently labeled PP7 phage coat proteins strongly associate to a
74 binding partner: an array of twenty-four PP7 mRNA stem-loops (PP7sl). In our settings,
75 this PP7 reporter construct is placed under the control of a promoter of interest and
76 integrated in the genome at the *GLT1* locus (Fig. 1b)³⁰, in a strain bearing a nuclear
77 tag (Hta2-mCherry) and expressing a fluorescently tagged PP7 protein (PP7 Δ FG-
78 GFPenvy^{31,32}, abbreviated PP7-GFP, Methods). Upon activation of the promoter, local
79 accumulation of newly synthesized transcripts at the Transcription Site (TS) leads to
80 the formation of a bright fluorescent focus due to the enrichment in PP7-GFP
81 fluorescence above the background signal (Fig. 1c and Supplementary Movie 1). The
82 fluorescence intensity at the TS is proportional to the number of mRNA being
83 transcribed and thus to the instantaneous load of RNA polymerases. After termination,
84 single mRNAs are exported out of the nucleus and their fast diffusion in the cytoplasm
85 prevents their detection under the selected illumination conditions.

86 Typically, time-lapses with fifteen-second intervals for twenty-five minutes with six Z-
87 planes for the PP7-GFP channel on four fields of view were performed. Image
88 segmentation and quantification were performed automatically, allowing to extract up
89 to four hundred single-cell traces for each experiment³³. The mean intensity of the 20
90 brightest pixels in the nucleus, from which the average cell fluorescence was

91 subtracted, was used as a measurement of TS intensity and thus as proxy for
92 transcriptional activity (Fig. 1d, Methods).

93 Fig. 1d displays the average TS fluorescence from more than 200 cells bearing the
94 p*STL1*-PP7sl reporter, following the activation of the HOG pathway by various NaCl
95 concentrations. The HOG-induced *STL1* promoter has been extensively studied at the
96 population and single cell level^{9,17,34,35}. As expected, increasing salt concentrations
97 lead to a proportionally increasing transcriptional output from the cell population,
98 whereas no change in TS fluorescence is detected in the control medium.

99 The hundreds of dynamic measurements acquired with the PP7 reporter form a rich
100 dataset where multiple features can be extracted from each single-cell trace (Fig. 1e,
101 Methods). Our automated image segmentation and analysis allow to reliably quantify
102 the appearance (Start Time) and disappearance (End Time) of the TS (Supplementary
103 Figure 2 and Method). The maximum intensity of the trace and the integral under the
104 curve provide estimates of the transcriptional output from each promoter (Fig. 1e). In
105 addition, transcriptional bursts can be identified by monitoring of strong fluctuations in
106 the TS intensity.

107 *Validation of the live mRNA reporter assay*

108 The mRNA dynamics measured with the PP7 assay are in close agreement with
109 previously reported data set^{34,36}. Nonetheless, we also verified with a dynamic protein
110 expression reporter that comparable results can be obtained (Supplementary Figure
111 3a). The dynamic Protein Synthesis Translocation Reporter (dPSTR) is an assay that
112 allows the kinetics of gene expression from a promoter of interest. It by-passes the
113 slow maturation time of fluorescent proteins (FP) by monitoring the relocation of the
114 fluorescent signal in the nucleus of the cell³⁷.

115 For the PP7 assay, as well as the dPSTR and many other expression reporters, an
116 additional copy of the promoter of interest is inserted in a non-native locus. In order to
117 address if this modified genomic environment alters the dynamics of gene expression,
118 we used CRISPR-Cas9 to integrate the PP7sl downstream of the endogenous *STL1*
119 promoter (Supplementary Figure 4). Interestingly, we observe only minor differences
120 between the p*STL1* at its endogenous location and at the *GLT1* locus. This observation

121 strongly suggests that the *STL1* promoter sequence placed at a non-endogenous locus
122 replicates many of the properties of the endogenous promoter.

123 *Intrinsic noise in osmostress-gene activation*

124 The microscopy images presented in Fig. 1c illustrate the noise that can be observed
125 in the activation of the p*STL1* promoter upon osmotic stress and which has been
126 previously reported^{9,17}. In order to verify that this noise is not due to a lack of activation
127 of the MAPK Hog1 in the non-responding cells, we combined the p*STL1*-PP7sl reporter
128 and the Hog1-mCherry relocation assay in the same strain. As expected, we observe
129 an absence of correlation between the two measurements (Supplementary Figure 5).
130 Indeed, cells with similar Hog1 relocation behaviors can display highly variable
131 transcriptional outputs.

132 An additional assay to observe this heterogeneity is to monitor the activation of two
133 *STL1* promoters within the same cell. Using a diploid strain where both *GLT1* loci were
134 modified with either a p*STL1*-24xPP7sl or a p*STL1*-24xMS2sl and expressing PP7-
135 mCherry and MS2-GFP proteins, we observe an uncorrelated activation of both loci
136 within each single cell (Supplementary Figure 6 and Supplementary Movie 2). This
137 observation confirms the high intrinsic noise generated by the *STL1* promoter upon
138 osmotic stress^{9,37}. The highly dynamic measurements provided by the PP7 reporter
139 allows us to decipher some of the parameters that contribute to this large variability.

140 *High variability in osmostress-genes transcription dynamics*

141 In addition to p*STL1*, five other stress-responsive promoters often used in the literature
142 to report on the HOG pathway transcriptional activity were selected for this study^{34,38}.
143 Each reporter strain differs only by the one thousand base pairs of the promoter
144 present in front of the PP7sl (800bp for p*STL1*, 660 for p*ALD3*^{9,39}); however, each
145 strain displays a different transcriptional response following a 0.2M NaCl stimulus (Fig.
146 2a). Because the level of accumulation of the PP7 signal at the transcription site and
147 the timing of the appearance and disappearance of the TS is different for each tested
148 promoter, it implies that the promoter sequence dictates multiple properties of the
149 transcription dynamics. These dynamic measurements are in general agreement with
150 control experiments performed with the dPSTR assay (Supplementary Figure 3b) and
151 previously published population-averaged data^{34,37}. Importantly, expressing three

152 times more phage coat proteins did not change the parameters extracted from the PP7
153 measurements for the two strongest promoters, denoting the absence of titration of
154 PP7-GFP reporter proteins in our experimental settings (Supplementary Figure 7).

155 The automated analysis allows to identify the presence or absence of a transcription
156 site in each single cell, and thus the fraction of cells that induce the promoter of interest
157 (Fig. 2b). Interestingly, even in absence of stimulus, some promoters display a basal
158 level of transcription. In the *pGRE2*, *pHSP12* and *pGPD1* reporter strains, an active
159 transcription site can be detected in 5 to 20% of the cells in the few time points before
160 the stimulus (Fig. 2c, Supplementary Movie 3). If the period of observation is extended
161 to a twenty-five-minute time lapse without stimulus, this fraction increases 2 to 3-folds
162 (Supplementary Figure 8). Upon activation by 0.2M NaCl, the fractions of responding
163 cells for the three promoters that display basal expression overcomes 85%, while it
164 remains below 65% for the three promoters without basal induction.

165 *Chromatin state sets the timing of transcription initiation*

166 A key parameter controlled by the promoter sequence is the timing of induction. In Fig.
167 2d, the time when cells become transcriptionally active (Start Time) is plotted as a
168 Cumulative Distribution Function (CDF) only for the cells where a TS is detected after
169 the stimulus, thereby excluding basal expressing cells and non-responding cells.
170 Treatment with 0.2M NaCl results in a sudden activation of transcription (Fig. 2d). This
171 contrasts with non-induced samples, where the CDF of the promoters displaying basal
172 activity rises almost linearly due to stochastic activation during the recording window
173 (Supplementary Figure 8c).

174 Upon stress, the promoters displaying basal activity are induced faster than the
175 promoters that are repressed under log-phase growth, with *pGPD1* being activated the
176 fastest (~1 min), while *pALD3* and *pSTL1* require more than 4 minutes for activation
177 (Fig. 2e). However, there is a great variability in transcription initiation between cells of
178 the same population, since we generally observe 3 to 4 minutes delay between the
179 10th and 90th percentiles, with the exception of *pGPD1* where the induction is more
180 uniform and less than 2 min delay is observed (Fig. 2e). Comparison between
181 individual replicates demonstrates the reliability of our measurement strategy.
182 Interestingly, we observe a positive correlation between faster transcriptional activation

183 from p*GPD1*, p*HSP12* and p*GRE2* and the presence of basal expression level. These
184 promoters also display the highest numbers of responding cells upon a 0.2M NaCl
185 shock. These results suggest that basal expression is associated with a more
186 permissive chromatin state, which enables a faster activation and higher probability of
187 transcription among the cell population.

188 To test this hypothesis, we disrupted the function of the SAGA chromatin remodeling
189 complex by deleting *GCN5*⁴⁰. As expected, we observe fewer transcribing cells and a
190 slower induction of the p*STL1* promoter in this background (Fig. 2f). Less remarkably,
191 abolishing histone H2AZ variants exchange at +1 and -1 nucleosomes by deleting
192 *HTZ1*⁴¹ only results in a reduced percentage of transcribing cells. Conversely,
193 chromatin state at the *STL1* promoter can be loosened by relieving the glucose
194 repression using raffinose as a C-source⁴². Interestingly, a fraction of the cells grown
195 in these conditions displays basal expression from the p*STL1*-PP7 reporter and the
196 Start Time in raffinose is accelerated by 1 min compared to glucose (Fig. 2g).

197 The link between the chromatin state under log-phase growth and the ability to induce
198 stress-responsive genes is confirmed by these results. A promoter that is tightly
199 repressed will need more Hog1 activity and thus more time to become transcriptionally
200 active, therefore displaying a lower fraction of responding cells.

201 *Early Hog1 activity dictates transcriptional competence*

202 The period of Hog1 activity provides a temporal window where transcription can
203 potentially be initiated. However, the switch to a transcriptionally active state takes
204 place almost exclusively within the first few minutes after the stimulus. When
205 comparing the characteristic timing of Hog1 nuclear enrichment to the CDF of Start
206 Times for cells bearing the p*STL1* reporter (Fig. 3a and Supplementary Figure 9a), we
207 observe that 90% of the transcribing cells initiate transcription during the first few
208 minutes of the stress response, while Hog1 nuclear accumulation rises and before it
209 drops below 80% of its maximum (decay time). A similar behavior is observed for all
210 the promoters tested, independently of the presence of basal levels (Fig. 3a and b).
211 For p*ALD3*, which is the slowest promoter tested, 87% of the Start Times are detected
212 before the decay of Hog1 activity (7 min) while the full adaptation time takes 14 min at
213 0.2M NaCl.

214 Interestingly, promoter output also decreases with the time after stimulus. Cells that
215 start transcribing *pSTL1* early display a larger integral over the PP7 signal and a higher
216 maximum intensity compared to cells that initiate transcription later (Fig. 3c and
217 Supplementary Figure 9b). A similar behavior is quantified for all tested promoters
218 (Supplementary Figures 9c and d). These measurements demonstrate that the high
219 Hog1 activity present in the first minutes of the response is key to determine both the
220 transcriptional state and overall output of the promoters.

221 *TFs control the dynamics and level of mRNA production*

222 Promoters dictate the timing of transcriptional activation of the ORF and the level at
223 which the mRNA is produced. To extract the transcriptional level of each promoter, we
224 use as a proxy the maximum of the PP7 trace of each single cell where a transcription
225 event could be detected (Fig. 4a). This value represents the maximal loading of
226 polymerases on the locus during the period of transcription. Similar results are
227 obtained when comparing the integral below the PP7 trace, which represents the total
228 transcriptional output from a promoter (Supplementary Figure 10a). As shown in Fig.
229 4a, each promoter has an intrinsic capability to induce a given level of transcription,
230 which is independent from the presence of basal transcription or the locus activation
231 time. Indeed, *pGRE2* displays the lowest level of induction among all tested promoters,
232 despite the presence of basal transcription and being the second-fastest promoter
233 activated.

234 As expected, the recruitment of the RNA polymerases is stimulated by the stress; the
235 three promoters with basal activities display a higher transcriptional level upon a 0.2M
236 NaCl stress than in normal growth conditions (Fig. 4b and Supplementary Figure 10b).
237 Both the general stress transcription factors Msn2 and Msn4 and the TFs activated by
238 the MAPK Hog1 (Hot1, Sko1, Smp1) contribute to the transcriptional up-
239 regulation^{29,38,43}. Based on studies on synthetic promoters, it has been established that
240 binding site number and distance from the Transcription Start Site (TSS) influence the
241 promoter output⁴⁴. Unfortunately, osmostress promoters display a wide diversity in
242 number and affinity of TF binding sites and no obvious prediction of the transcriptional
243 activity can be drawn (Supplementary Figure 11). While multiple Msn2/4 binding sites

244 can be found on the *GPD1* and *STL1* promoter sequences, their activation are only
245 mildly affected by deletions of these two TFs (Supplementary Figure 12).

246 Both *GPD1* and *STL1* are primarily Hog1 targets^{28,29,38}. However, their requirements
247 for Hog1 activity is strikingly different. In strains where the MAPK has been anchored
248 to the plasma membrane to limit its nuclear enrichment⁴⁵, p*STL1* induction is virtually
249 abolished (only 1.5% transcribing cells) while p*GPD1* activity is barely affected
250 (Supplementary Figure 13). Similarly, deletion of either TF Sko1 or Hot1 profoundly
251 alter the capacity of p*STL1* to be induced (Fig. 4c -f) while these same mutations have
252 a weaker effect on the *GPD1* promoter.

253 Because the induction of the *STL1* promoter requires an efficient chromatin
254 remodeling, every defect (TF deletion or absence of Hog1 in the nucleus) strongly
255 alters its capability to induce transcription. In comparison, the p*GPD1* is less perturbed
256 by these same defects. We postulate that TFs act in a cooperative manner on p*STL1*,
257 while they act independently of each other on p*GPD1*.

258 *Bursts of PolII transcription in osmostress-gene activation*

259 The PP7 and MS2 systems have allowed to directly visualize transcriptional bursting.
260 In order to identify bursts arising from osmostress promoters, we sought to detect
261 strong fluctuations in each single-cell trace. Fluctuations in TS intensities were filtered
262 to retain only peaks separated by pronounced troughs (Methods). In 20 to 30% of the
263 traces, two or more peaks are identified (Fig. 5a and b). The total length of the
264 transcript downstream of the promoter is 8kb (1.5kb for the stem loops + 6.5kb for
265 *GLT1*). Based on a transcription speed of 20bp/s³⁰, the expected lifetime of a transcript
266 at the TS is 6.6 min. This corresponds well to the mean duration observed for the
267 p*ALD3*, p*CTT1*, p*STL1* and p*GRE2* reporters (Fig. 5c). However, it is unlikely that the
268 strong TS intensities recorded are generated by a single transcript, but rather by a
269 group of RNA PolII that simultaneously transcribe the locus, probably forming convoys
270 of polymerases⁴⁶. Indeed, single mRNA FISH experiments have shown that following
271 a 0.2M NaCl stress, the endogenous *STL1* locus produces on average 20 mRNAs per
272 cell, with some cells producing up to 100³⁶.

273 For p*HSP12* and p*GPD1*, the average peak duration is longer than 11 min (Fig. 5c),
274 suggesting that multiple convoys of polymerases are traveling consecutively through

275 the ORF. Unfortunately, the long half-lives of the transcripts on the locus prevent a
276 separation of individual groups of polymerases. However, when we achieve to isolate
277 individual peaks in the single cell traces, their duration becomes closer to the expected
278 value of 6.6 min (Fig. 5d). In addition, the output of the transcription estimated by the
279 maximum intensity of the trace or the integral under the whole curve is equal or lower
280 for traces with multiple pulses compared to traces where only a single peak is present
281 (Fig. 5e and Supplementary Figure 14). Together these data strengthen the notion that
282 these stress-responsive promoters are highly processive, displaying an elevated rate
283 of transcription once activated. Only brief pauses in the transcription can be observed
284 in a small fraction of the responding cells.

285 *MAPK activity opens an opportunity window for transcription*

286 We have shown that transcription initiation is dictated by early Hog1 activity. Next, we
287 want to assess what the determinants of transcription shutoff are and by extension,
288 the duration of transcriptional activity. In the HOG pathway, the duration of transcription
289 has been reported to be limited by the cellular adaptation time^{34,38}. Therefore, the
290 duration of transcription is shorter after a 0.1M NaCl stress and longer after a 0.3M
291 stress, compared to a 0.2M stress (Fig. 6a). For the p*STL1* promoter, the last time
292 point where a PP7 signal is detected at the TS matches the timing of nuclear exit of
293 the MAPK at all concentrations tested (Fig. 6b).

294 In order to challenge this link between Hog1 activity and transcriptional arrest, we
295 sought to modulate the MAPK activity pattern by controlling the cellular environment in
296 a dynamic manner. Using a flow channel set-up, we generated a step, a pulse, or a
297 ramp in NaCl concentrations (Fig. 6c, Methods). These experiments were performed
298 in a strain carrying the p*STL1*-PP7sl reporter in conjunction with Hog1-mCherry,
299 allowing to monitor kinase activity and the downstream transcriptional response in the
300 same cell.

301 The step stimulus at 0.2M NaCl mimics the experiments performed in wells, where the
302 concentration of the osmolyte is suddenly increased at time zero and remains constant
303 throughout the experiments (Supplementary Movie 4). The mean responses at the
304 population level (Fig. 6c) confirm this relationship between Hog1 adaptation time and
305 transcription shutoff time. However, at the single cell level, no direct correlation is

306 observed between these two measurements due to important single cell variability (Fig.
307 6f).

308 In the pulse assay, 7 min after the initial 0.2M step, the NaCl concentration is set back
309 to 0M (Supplementary Movie 5). This shortens the MAPK activity period, as Hog1
310 leaves the nucleus immediately when cells are brought back in the normal growth
311 medium. Removing the kinase from the nucleus has a direct impact on the
312 transcriptional process. First, fewer cells become transcriptionally active. Second, the
313 active TS sites disappear within a few minutes after the end of the pulse (Fig. 6d and
314 e). Therefore in this context, we observe a direct correlation between Hog1 activity and
315 transcription, which is in line with the known role played by MAPKs, and Hog1 in
316 particular, on multiple steps of the transcriptional process^{47,48}.

317 The ramp experiment starts with a pulse at 0.2M NaCl followed by a slow increase of
318 the NaCl concentration up to 0.6M over the next 20 min (Supplementary Movie 6). This
319 constant rise in external osmolarity extends the Hog1 activity window by preventing
320 the adaptation of the cells. More cells can become transcriptionally active and the
321 transcription shut off is delayed (Fig. 6d and e). However, in these conditions, there is
322 a clear lack of correlation between Hog1 activity, which is sustained in many cells over
323 the 30min of the time-lapse, and the transcription output of the *pSTL1* that stops much
324 earlier. Taken together, these experiments demonstrate that the MAPK activity is
325 required but not sufficient to sustain the transcriptional process. In the ramp
326 experiment, transcription cannot be sustained throughout the whole Hog1 activity
327 window, demonstrating that other factors contribute to limiting the duration of the
328 transcription.

329 *Promoter identity influences the transcription shutoff time*

330 In order to test whether the promoter identity plays a role in the process of transcription
331 shutoff, we quantified the duration of the transcriptional period for the six promoters
332 and plotted the cumulative distribution of End Times following a 0.2M NaCl stress (Fig.
333 7a and b). Interestingly, despite similar cell volume adaptation time for all the
334 experiments, the promoters display substantially different kinetics of inactivation.
335 Promoters transcribing at a lower level (*pCTT1* and *pGRE2*) terminate transcription
336 earlier. This shorter transcriptional window may reflect an inferior recruitment of

337 transcriptional activators to the promoter, enabling an earlier inhibition of transcription
338 due to chromatin closure. In addition, promoters with basal activity display an extended
339 period of transcription after adaptation (Fig. 7a and b). For *pGPD1* and *pGRE2*, this
340 results in a biphasic decay, where the first phase corresponds to the arrest of Hog1-
341 induced transcription and the second phase can be associated to the basal
342 transcription arising from these promoters (Fig. 7b). Note that basal transcription may
343 even be increased due to a higher basal Hog1 signaling activity post high osmolarity
344 conditions⁴⁹.

345 Remarkably, *pHSP12* transcription persists beyond the adaptation time, with nearly
346 30% of the cells displaying an active TS at the end of the experiment. This suggests
347 that basal expression from this promoter is strongly increased post-stimulus. In
348 contrast to *pGPD1* and *pGRE2*, *pHSP12* possesses numerous Msn2/4 binding sites.
349 Although the relocation dynamics of Hog1 and Msn2 are highly similar during the
350 adaptation phase, Msn2 displays some stochastic secondary pulses²⁷, that are not
351 correlated to Hog1 relocation events. This could explain the stronger basal expression
352 arising from this promoter post-adaptation (Supplementary Figure 1e and f).

353 To summarize, these measurements demonstrate that the pattern of MAPK activity
354 provides a temporal window where transcription can take place. When the signaling
355 cascade is shut off, transcription ceases soon afterward. However, the promoter
356 identity, and probably its propensity to recruit positive activators, will determine for how
357 long it can sustain an open chromatin environment favorable to transcription before
358 Hog1 activity decreases due to cellular adaptation.

359 **Discussion**

360 In this study, we have constructed PP7 reporter strains to monitor the transcription
361 dynamics of osmostress promoters. The second exogenous copy of the promoter is
362 integrated at the *GLT1* locus. This strategy provides a similar genomic environment for
363 all the promoters, in order to compare their specific characteristics. Interestingly, we
364 saw only minor differences in CDF of Start Times of the *pSTL1* when integrated at its
365 endogenous locus compared to the *GLT1* locus. This observation provides a strong
366 evidence that TF binding and chromatin state of the duplicated promoter sequences

367 mimic closely the ones at the native environment of the gene. Note that the signal at
368 the TS is expected to be proportional to the length of the transcribed mRNA. The *GLT1*
369 locus with its 6.5kB length was expected to provide a signal four times stronger than
370 the endogenous *STL1* ORF (1.7kB). The unexpectedly high signal obtained from the
371 PP7 reporter at the endogenous locus may be indicative of global difference in
372 transcription rates between the *GLT1* and *STL1* ORFs alternatively, the smaller *STL1*
373 ORF might enhance transcription efficiency via gene-looping^{50,51}.

374 Our data illustrate the complex balance that exists between positive and negative
375 regulators taking place at the stress induced loci. At each locus, positive and negative
376 regulators will control the level and duration of transcription. We have shown that the
377 first few minutes of Hog1 activity are essential to initiate the transcription. Transcription
378 factors, chromatin remodelers such as the SAGA and RSC complexes, together with
379 Hog1 will contribute to open and maintain an accessible chromatin environment at the
380 stress-response loci^{35,40}. Once initiated, transcription seems highly processive and
381 only in a small fraction of traces, we are able to detect a pause in transcription.
382 However, it has been shown that PolII recruits additional chromatin remodelers,
383 including the Ino80 complex and Asf1 that will redeposit nucleosomes after acute
384 transcription⁵². These conflicting activities will determine the overall duration of
385 transcription at a locus. Indeed, promoters with lower transcriptional activity, such as
386 *pGRE2* and *pCTT1*, recruit fewer positive activators and will be repressed faster by the
387 negative regulators.

388 The repression level of a promoter during log-phase growth will determine the speed
389 and the noise of the transcription activation process. Thus, for each promoter, a trade-
390 off has to be found between these two contradictory requirements. For instance,
391 *GPD1*, which is essential for survival to osmotic stress, has an important basal
392 expression level and can thus be rapidly induced upon stress. Interestingly, the
393 chromatin state, encoded in part by the promoter sequence, can be tuned by external
394 growth conditions. Thus, the noise generated by a promoter is not rigidly set by its DNA
395 sequence but fluctuate based on the environment.

396 In higher eukaryotes, the stress response MAPKs p38 and JNK relocate to the nucleus
397 upon activation^{53,54}. Early genes such as c-Fos or c-Jun, are induced within minutes

398 after activation of signaling^{3,55}. Interestingly, these loci display basal expression and
399 require minimal chromatin modification for their induction^{56,57}. Conversely, delayed
400 primary response and secondary response genes require more chromatin remodeling
401 to induce their activation^{55,58}. These similarities with Hog1-gene transcriptional
402 regulation suggest a high conservation in the mechanisms used by MAPK in
403 eukaryotes to regulate the dynamics of gene expression.

404 **Methods**

405 *Plasmids and yeast strains*

406 Plasmids and yeast strains used in this study are listed in Supplementary Tables 1 and
407 2. All strains were constructed in the W303 background. Transformations were
408 performed with standard lithium-acetate protocols. Gene deletions and gene tagging
409 were performed with either pFA6a cassettes^{59,60} or pGT cassettes⁶¹. Transformants
410 were selected with auxotrophy markers (Uracil, Histidine, Leucine, Tryptophan,
411 Adenine) and gene deletions were performed with antibiotic resistance to
412 Nourseothricin (NAT) or Kanamycin (KAN). In order to generate the membrane
413 anchored Hog1, the pGTT-mCherry vector was modified by inserting annealed oligos
414 encoding the last 30bp of the Ras2 sequence to obtain the pGTT-mCherry-CaaX
415 plasmid. A strain possessing the Hog1-mCherry:*LEU2* modification was transformed
416 with the pGTT-mCherry-CaaX plasmid linearized with *Xba*I and *Sac*I to induce a
417 marker switch and introduce the membrane anchoring motif.

418 *PP7 and MS2 strains construction*

419 The PP7-GFP plasmids are based on the bright and photostable GFPenvy fluorescent
420 protein³². The PP7 protein was derived from Larson et al.³⁰ (Addgene# 35194) with a
421 truncation in the capsid assembly domain (PP7 Δ FG residues 67–75: CSTSVCGE³¹).
422 The expression of the PP7 construct is controlled by an *ADH1* promoter and a *CYC1*
423 terminator. The final construct pVW284 is cloned in a Single Integration Vector URA3
424 (pSIVu⁶¹). The PP7-mCherry was cloned by replacing the GFP by the mCherry
425 sequence. The MS2-GFP was generated by using the original MS2 sequence from
426 Bertrand et al.¹⁸, which also lacks the capsid assembly domain (Addgene# 27117),
427 inserted into the pVW284. The PP7 stem-loops plasmids are based on the previously

428 published *pPOL1 24xPP7sl* integrative plasmid³⁰ (Addgene #35196). The stress
429 responsive promoters replace the *POL1* promoter in the original construct using 1kb
430 (0.8kb for *pSTL1*, 0.66kb for *pALD3*) upstream of the start codon. The *pSTL1-*
431 *24xMS2sl* was generated by replacing the PP7sl with the MS2 stem loops obtained
432 from Bertrand et al.¹⁸ (Addgene# 31865).

433 A strain bearing the Hta2-mCherry nuclear marker and expressing the PP7-GFP was
434 transformed with plasmids containing the different osmostress promoters driving the
435 PP7sl expression, linearized with a *NotI* digestion and integrated upstream of the *GLT1*
436 ORF, as previously published³⁰. Correct integration into the *GLT1* locus was screened
437 by colony PCR with primers in the *GLT1* ORF (+600 bp) and in the *TEF* terminator of
438 the selection marker on genomic DNA extractions. The integrity of the PP7 stem-loops
439 array was assessed with primers within the *TEF* terminator and in *GLT1* ORF (+250
440 bp) for all the promoters and deletions, after each transformation performed. For all the
441 strains used in the study, at least two clones with correct genotypes were isolated and
442 tested during a salt challenge time-lapse experiment. From the data analysis, the most
443 frequent phenotype was isolated and the strain selected.

444 To tag the endogenous locus of *STL1* with the 24xPP7sl, the plasmid pSP264 with the
445 *STL1* promoter was modified by replacing the *GLT1* ORF sequence by a 500bp
446 sequence starting 100 bp after the start codon of *STL1*. The plasmid was digested
447 *SacI-NotI* and purified over a gel to isolate a fragment that contains the *pSTL1-*
448 *24xPP7sl-STL1*₁₀₀₋₆₀₀. A double-strand break was generated in the *STL1* ORF using
449 Cas9 and a sgRNA targeting the PAM motif GGG 62 bp upstream of the start codon.
450 The Cas9 and sgRNA are expressed from a 2μ plasmid (Addgene # 35464⁶²) slightly
451 modified from the work from Laughery et al. (Addgene# 67639⁶³). The purified DNA
452 fragment containing the stem-loops was used as repair DNA to promote homologous
453 recombination at the *STL1* locus (Supplementary Figure 4a). The correct size of the
454 inserted fragment was verified by colony PCR around the PP7sl insert. Multiple positive
455 clones were screened by microscopy. The results from two transformants are
456 presented in this work to ensure that potentially undesired DNA alterations by Cas9 do
457 not affect the response in the HOG pathway.

458 In order to generate the diploid reporter strain, a MAT α strain containing the PP7-
459 mCherry::*URA3*, p*STL1* 24xPP7sl:*GLT1* and Hta2-tdiRFP:*TRP1* was crossed to a
460 MAT α strain bearing the MS2-GFP::*URA3*, p*STL1* 24xMS2sl:*GLT1* and Hta2-
461 tdiRFP:*NAT*. Haploid cells were mixed on a YPD plate for a few hours before cells
462 were resuspended in water and spread with beads on a selection plate (SD-TRP
463 +NAT).

464 The plasmids generated for this study are available on Addgene.

465 *Yeast culture*

466 Yeast cells were grown in YPD medium (YEP Broth: CCM0405, ForMedium) for
467 transformation or in Synthetic Defined (SD) medium (YNB:CYN3801/CSM: DCS0521,
468 ForMedium) for microscopy experiments. Before time-lapse experiments, cells were
469 grown at least 24 hours in log-phase. A saturated overnight culture in SD medium was
470 diluted into fresh SD-full medium to OD₆₀₀ 0.025 in the morning and grown for roughly
471 8 hours to reach OD₆₀₀ 0.3-0.5. In the evening, cultures were diluted by adding
472 (0.5/OD₆₀₀) μ l of cultures in 5ml SD-full for an overnight growth that kept cells in log-
473 phase conditions. Cultures reached an OD₆₀₀ of 0.1-0.3 in the morning of the second
474 day and were further diluted when necessary to remain below an OD₆₀₀ of 0.4 during
475 the day. To prepare the samples, these log-phase cultures were further diluted to an
476 OD₆₀₀ 0.05 and sonicated twice 1min (diploids were not sonicated) before placing 200
477 μ l of culture into the well of a 96-well glass bottom plate (MGB096-1-2LG, Matrical
478 Bioscience) previously coated with a filtered solution of Concanavalin A diluted to
479 0.5mg/ml in water (C2010, Sigma-Aldrich)⁶⁴. Cells were let to settle for 30–45 minutes
480 before imaging. Osmotic shock was performed under the microscope, by adding 100
481 μ l of a three times concentrated SD-full+NaCl stock solutions to the 200 μ l of medium
482 already in the well, to reach the final desired salt concentration.

483 *Microscopy*

484 Images were acquired on a fully automated inverted epi-fluorescence microscope (Ti2-
485 Eclipse, Nikon) placed in an incubation chamber set at 30°C. Excitation was provided
486 by a solid-state light source (SpectraX, Lumencor) and dedicated filter sets were used
487 to excite and detect the proper fluorescence wavelengths with a sCMOS camera
488 (Flash 4.0, Hamamatsu). A motorized XY-stage was used to acquire multiple fields of

489 views in parallel and a piezo Z-stage (Nano-Z200, Mad City Labs) allowed fast Z-
490 dimension scanning. Micro-manager was used to control the multidimensional
491 acquisitions⁶⁵.

492 Experiments with PP7sl were acquired with a 60X oil objective. For strains with PP7-
493 GFP and Hta2-mCherry, GFP (40ms, 3% LED power) and RFP (20ms), along with two
494 bright field images were recorded every 15 seconds for the GFP and every minute for
495 the other channels, for a total duration of 25 minutes. Six z-stacks were performed on
496 the GFP channels covering $\pm 1.2 \mu\text{m}$ from the central plane with $0.4 \mu\text{m}$ steps. An
497 average bleaching of 32% for the GFP and 26% for the RFP for the whole time-lapse
498 was quantified in a strain without the PP7 stem-loops, to avoid artifacts from the
499 appearance of bright fluorescent foci. For all time-lapse experiments, media addition
500 was performed before time point 4, defined as time zero. All microscopy experiments
501 were performed in duplicate for non-induced control experiment and at least triplicate
502 for the NaCl induced experiments.

503 *Flow chamber experiments*

504 The flow experiments were performed in Ibidi chambers (μ -Slide VI 0.4, Ibidi). Two
505 50ml Falcon tube reservoirs containing SD-full + $0.5 \mu\text{g/ml}$ fluorescein-dextran (D3305,
506 ThermoFischer) and SD-full + 0.6 M NaCl were put under a pressure of 30mbar
507 (FlowEZ, Fluigent). The media coming from each reservoir were connected using FEP
508 tubing ($1/16''$ OD x $0.020''$ ID, Fluigent) to a 3-way valve (2-switch, Fluigent). The
509 concentration of NaCl in the medium was controlled using a Pulse-Width Modulation
510 strategy^{66,67}. Periods of 4 seconds were used and within this time, the valve controlled
511 the fraction of time when SD-full versus SD-full + NaCl was flowing. TTL signals
512 generated by an Arduino Uno board and dedicated scripts were used to control
513 precisely the switching of the valve. The fluorescein present in the SD-full medium
514 quantified outside the Cell object provided an estimate of the NaCl concentration in the
515 medium. Some strong fluctuations in this signal were probably generated by dust
516 particles in the imaging oil or FLSN-dextran aggregates in the flow chamber. Following
517 24hrs log-phase growth, cells bearing the pSTL1-PP7sl reporter, Hog1-mCherry and
518 Hta2-tdiRFP tags were diluted to OD 0.2, briefly sonicated and loaded in the ibidi

519 channel previously coated by Concanavalin A. Cells were left to settle in the channel
520 for 10 minutes before SD-full flow was started.

521 *Raffinose experiment*

522 For the experiments comparing pSTL1-PP7sl induction in glucose versus raffinose,
523 cells were grown overnight to saturation in SD-full medium. The cultures were diluted
524 to OD 0.025 (Glucose) or 0.05 (Raffinose) and grown at 30°C for at least four hours.
525 In the raffinose medium, the expression level of the PP7-GFP was 2-fold lower than in
526 glucose. Because of this low fluorescence intensity, cells were imaged with a 40X
527 objective, and a single Z-plane was acquired. Manual curation of the images was
528 performed to define the Start Time in more than 250 cells. This experiment was
529 performed in duplicate.

530 *Data analysis*

531 Time-lapse movies were analyzed in an automated way: cell segmentation, tracking
532 and feature measurements were performed by the YeastQuant platform³³. Summary
533 of the dataset, strains and cell numbers are provided in Supplementary Table 3. All
534 PP7 experiments were realized in at least two or three fully independent replicate
535 experiments. A representative experiment was selected for each strain and inducing
536 conditions, based on cell size and cell adaptation dynamics. The replicates which did
537 not pass one of these controls were discarded from the replicate analyses. Individual
538 single-cell traces were filtered based on cell shape and GFP intensity to remove
539 segmentation errors or other experimental artifacts. In addition, cells in mitosis were
540 removed from the analysis with a 0.95 filter on the nuclei eccentricity, to remove
541 artifacts from locus and PP7 signal duplication.

542 The Hta2 signal combined with the two bright field images allowed to define the
543 nucleus and cell borders. The GFP z-stacks were converted by a maximum intensity
544 projection in a single image that was used for quantification. In order to avoid improper
545 quantification of transcription sites at the nuclear periphery, the Nucleus object defined
546 by the histone fluorescence was expanded by 5 pixels within the Cell object to define
547 the ExpNucl object. The transcription site intensity was quantified by the difference
548 between the mean intensity of the 20 brightest pixels in the ExpNucl (HiPix) and the
549 median intensity from the whole cell. This provides a continuous trace which is close

550 to zero in absence of TS and increases by up to few hundred counts when a TS is
551 present. To identify the presence of a transcription site, a second feature named
552 ConnectedHiPix was used (Supplementary Figure 2a). Starting from the 20 HiPix, a
553 morphological opening of the image was performed to remove isolated pixels and
554 retaining only the ones that clustered together which correspond to the transcription
555 site. The ConnectedHiPix value was set to the mean intensity of the pixel present in
556 the largest object remaining after the morphological operation. If no pixel remained
557 after the morphological operation, the ConnectedHiPix was set to NaN. In each single-
558 cell trace, ConnectedHiPix values only detected for a single time point were removed.
559 After this filtering, the first and last time points where a ConnectedHiPix was measured
560 were defined as transcription initiation (Start Time) and shutoff (End Time),
561 respectively. Manual curation of Start and End Times from raw microscopy images
562 was performed to validate this transcription site detection strategy (Supplementary
563 Figure 2b and c). In order to detect individual transcriptional bursts in the HiPix traces,
564 the *findpeak* algorithm was used to identify in the trace all the peaks larger than a
565 threshold of 7 counts within the Start and End Times. Following this first process, a set
566 of conditions were defined to retain only the more reliable fluctuations: the drop
567 following the peak has to be larger the fourth of the peak intensity; the intensity of the
568 following peak has to rise by more than a third of the value at the trough. In addition,
569 the value of the peak has to be at least one fifth of the maximum intensity of the trace
570 in order to remove small intensity fluctuations being considered as peaks.

571 *Data Availability*

572 Source data for Figures 1d, 2a, 2f,2g, 3a, 4b, 4c, and 6c and Supplementary Figures
573 1, 4, 5, 6, 8, 12, 13 are provided with the paper. The raw images and additional features
574 measurements that support the findings of this study are available from the
575 corresponding author upon reasonable request.

576 *Code Availability*

577 The image analysis platform has been published previously³³. A more recent version
578 of the code can be obtained from the corresponding author. A script to extract
579 measured parameters from the data is provided as a supplementary file.

580

581

582 References

- 583 1. Gasch, A. P. *et al.* Genomic expression programs in the response of yeast cells to
584 environmental changes. *Mol Biol Cell* **11**, 4241–4257 (2000).
- 585 2. Roberts, C. J. *et al.* Signaling and circuitry of multiple MAPK pathways revealed by a matrix
586 of global gene expression profiles. *Science* **287**, 873–880 (2000).
- 587 3. Ferreiro, I. *et al.* Whole genome analysis of p38 SAPK-mediated gene expression upon
588 stress. *BMC Genomics* **11**, 144 (2010).
- 589 4. Berry, D. B. & Gasch, A. P. Stress-activated genomic expression changes serve a
590 preparative role for impending stress in yeast. *Mol Biol Cell* **19**, 4580–4587 (2008).
- 591 5. Chen, R. E., Patterson, J. C., Goupil, L. S. & Thorner, J. Dynamic localization of Fus3
592 mitogen-activated protein kinase is necessary to evoke appropriate responses and avoid
593 cytotoxic effects. *Mol Cell Biol* **30**, 4293–4307 (2010).
- 594 6. Formstecher, E. *et al.* PEA-15 Mediates Cytoplasmic Sequestration of ERK MAP Kinase.
595 *Developmental Cell* **1**, 239–250 (2001).
- 596 7. Raser, J. M. & O’Shea, Erin K. Control of stochasticity in eukaryotic gene expression.
597 *Science* **304**, 1811–1814 (2004).
- 598 8. Colman-Lerner, A. *et al.* Regulated cell-to-cell variation in a cell-fate decision system.
599 *Nature* **437**, 699–706 (2005).
- 600 9. Pelet, S. *et al.* Transient activation of the HOG MAPK pathway regulates bimodal gene
601 expression. *Science* **332**, 732–735 (2011).
- 602 10. Corrigan, A. M. & Chubb, J. R. Regulation of Transcriptional Bursting by a Naturally
603 Oscillating Signal. *Current Biology* **24**, 205–211 (2014).
- 604 11. Roux, P. P. & Blenis, J. ERK and p38 MAPK-Activated Protein Kinases: a Family of Protein
605 Kinases with Diverse Biological Functions. *Microbiology and Molecular Biology Reviews*
606 **68**, 320–344 (2004).
- 607 12. Chen, R. E. & Thorner, J. Function and regulation in MAPK signaling pathways: lessons
608 learned from the yeast *Saccharomyces cerevisiae*. *Biochim Biophys Acta* **1773**, 1311–
609 1340 (2007).
- 610 13. Saito, H. & Posas, F. Response to hyperosmotic stress. *Genetics* **192**, 289–318 (2012).
- 611 14. Hohmann, S., Krantz, M. & Nordlander, B. Yeast osmoregulation. *Meth Enzymol* **428**, 29–
612 45 (2007).
- 613 15. de Nadal, E. & Posas, F. Multilayered control of gene expression by stress-activated
614 protein kinases. *EMBO J* **29**, 4–13 (2010).
- 615 16. de Nadal, E., Ammerer, G. & Posas, F. Controlling gene expression in response to stress.
616 *Nat Rev Genet* **12**, 833–845 (2011).
- 617 17. Neuert, G. *et al.* Systematic Identification of Signal-Activated Stochastic Gene Regulation.
618 *Science* **339**, 584–587 (2013).
- 619 18. Bertrand, E. *et al.* Localization of ASH1 mRNA particles in living yeast. *Mol Cell* **2**, 437–
620 445 (1998).
- 621 19. Buxbaum, A. R., Haimovich, G. & Singer, R. H. In the right place at the right time:
622 visualizing and understanding mRNA localization. *Nat Rev Mol Cell Biol* **16**, 95–109
623 (2015).
- 624 20. Urbanek, M. O., Galka-Marciniak, P., Olejniczak, M. & Krzyzosiak, W. J. RNA imaging in
625 living cells – methods and applications. *RNA Biology* **11**, 1083–1095 (2014).
- 626 21. Lionnet, T. & Singer, R. H. Transcription goes digital. *EMBO Rep* **13**, 313–321 (2012).
- 627 22. Fritzsich, C. *et al.* Estrogen-dependent control and cell-to-cell variability of transcriptional
628 bursting. *Molecular Systems Biology* **14**, e7678 (2018).

- 629 23. Zoller, B., Little, S. C. & Gregor, T. Diverse Spatial Expression Patterns Emerge from
630 Unified Kinetics of Transcriptional Bursting. *Cell* **175**, 835–847.e25 (2018).
- 631 24. Reiser, V., Ruis, H. & Ammerer, G. Kinase activity-dependent nuclear export opposes
632 stress-induced nuclear accumulation and retention of Hog1 mitogen-activated protein
633 kinase in the budding yeast *Saccharomyces cerevisiae*. *Mol Biol Cell* **10**, 1147–1161
634 (1999).
- 635 25. Muzzey, D., Gómez-Urbe, C. A., Mettetal, J. T. & van Oudenaarden, A. A systems-level
636 analysis of perfect adaptation in yeast osmoregulation. *Cell* **138**, 160–171 (2009).
- 637 26. Görner, W. *et al.* Nuclear localization of the C2H2 zinc finger protein Msn2p is regulated
638 by stress and protein kinase A activity. *Genes Dev.* **12**, 586–597 (1998).
- 639 27. Hao, N. & O’Shea, E. K. Signal-dependent dynamics of transcription factor translocation
640 controls gene expression. *Nature Structural & Molecular Biology* **19**, 31–39 (2012).
- 641 28. O’Rourke, S. M. & Herskowitz, I. Unique and Redundant Roles for HOG MAPK Pathway
642 Components as Revealed by Whole-Genome Expression Analysis. *Mol Biol Cell* **15**, 532–
643 542 (2003).
- 644 29. Capaldi, A. P. *et al.* Structure and function of a transcriptional network activated by the
645 MAPK Hog1. *Nat Genet* **40**, 1300–1306 (2008).
- 646 30. Larson, D. R., Zenklusen, D., Wu, B., Chao, J. A. & Singer, R. H. Real-Time Observation
647 of Transcription Initiation and Elongation on an Endogenous Yeast Gene. *Science* **332**,
648 475–478 (2011).
- 649 31. Chao, J. A., Patskovsky, Y., Almo, S. C. & Singer, R. H. Structural basis for the coevolution
650 of a viral RNA–protein complex. *Nat. Struct. Mol. Biol.* **15**, 103–105 (2007).
- 651 32. Slubowski, C. J., Funk, A. D., Roesner, J. M., Paulissen, S. M. & Huang, L. S. Plasmids
652 for C-terminal tagging in *Saccharomyces cerevisiae* that contain improved GFP proteins,
653 Envy and Ivy. *Yeast* **32**, 379–387 (2015).
- 654 33. Pelet, S., Dechant, R., Lee, S. S., van Drogen, F. & Peter, M. An integrated image analysis
655 platform to quantify signal transduction in single cells. *Integrative biology: quantitative*
656 *biosciences from nano to macro* **4**, 1274–1282 (2012).
- 657 34. de Nadal, E. *et al.* The MAPK Hog1 recruits Rpd3 histone deacetylase to activate
658 osmoreponsive genes. *Nature* **427**, 370–374 (2004).
- 659 35. Mas, G. *et al.* Recruitment of a chromatin remodelling complex by the Hog1 MAP kinase
660 to stress genes. *EMBO J* **28**, 326–336 (2009).
- 661 36. Li, G. & Neuert, G. Multiplex RNA single molecule FISH of inducible mRNAs in single yeast
662 cells. *Sci Data* **6**, 94 (2019).
- 663 37. Aymoz, D., Wosika, V., Durandau, E. & Pelet, S. Real-time quantification of protein
664 expression at the single-cell level via dynamic protein synthesis translocation reporters.
665 *Nature Communications* **7**, 11304 (2016).
- 666 38. Rep, M. *et al.* Osmotic stress-induced gene expression in *Saccharomyces cerevisiae*
667 requires Msn1p and the novel nuclear factor Hot1p. *Mol Cell Biol* **19**, 5474–5485 (1999).
- 668 39. Alepuz, P. M., de Nadal, E., Zapater, M., Ammerer, G. & Posas, F. Osmostress-induced
669 transcription by Hot1 depends on a Hog1-mediated recruitment of the RNA Pol II. *EMBO*
670 *J* **22**, 2433–2442 (2003).
- 671 40. Zapater, M., Sohrmann, M., Peter, M., Posas, F. & de Nadal, E. Selective requirement for
672 SAGA in Hog1-mediated gene expression depending on the severity of the external
673 osmostress conditions. *Mol Cell Biol* **27**, 3900–3910 (2007).
- 674 41. Wan, Y. *et al.* Role of the histone variant H2A.Z/Htz1p in TBP recruitment, chromatin
675 dynamics, and regulated expression of oleate-responsive genes. *Mol Cell Biol* **29**, 2346–
676 2358 (2009).
- 677 42. Ferreira, C. & Lucas, C. Glucose repression over *Saccharomyces cerevisiae* glycerol/H⁺
678 symporter gene STL1 is overcome by high temperature. *FEBS Lett* **581**, 1923–1927
679 (2007).
- 680 43. de Nadal, E. & Posas, F. Regulation of gene expression in response to osmostress by the
681 yeast stress-activated protein kinase Hog1. *Topics in Current Genetics* **20**, 81 (2008).

- 682 44. Sharon, E. *et al.* Inferring gene regulatory logic from high-throughput measurements of
683 thousands of systematically designed promoters. *Nat Biotechnol* **30**, 521–530 (2012).
- 684 45. Westfall, P. J., Patterson, J. C., Chen, R. E. & Thorner, J. Stress resistance and signal
685 fidelity independent of nuclear MAPK function. *Proc Natl Acad Sci USA* **105**, 12212–12217
686 (2008).
- 687 46. Tantale, K. *et al.* A single-molecule view of transcription reveals convoys of RNA
688 polymerases and multi-scale bursting. *Nat Commun* **7**, 12248 (2016).
- 689 47. Pokholok, D. K., Zeitlinger, J., Hannett, N. M., Reynolds, D. B. & Young, R. A. Activated
690 signal transduction kinases frequently occupy target genes. *Science* **313**, 533–536 (2006).
- 691 48. Proft, M. *et al.* The stress-activated Hog1 kinase is a selective transcriptional elongation
692 factor for genes responding to osmotic stress. *Mol Cell* **23**, 241–250 (2006).
- 693 49. Macia, J. *et al.* Dynamic signaling in the Hog1 MAPK pathway relies on high basal signal
694 transduction. *Science Signaling* **2**, ra13 (2009).
- 695 50. O’Sullivan, J. M. *et al.* Gene loops juxtapose promoters and terminators in yeast. *Nat*
696 *Genet* **36**, 1014–1018 (2004).
- 697 51. Ansari, A. A role for the CPF 3’-end processing machinery in RNAP II-dependent gene
698 looping. *Genes & Development* **19**, 2969–2978 (2005).
- 699 52. Klopff, E. *et al.* Cooperation between the INO80 complex and histone chaperones
700 determines adaptation of stress gene transcription in the yeast *Saccharomyces cerevisiae*.
701 *Mol Cell Biol* **29**, 4994–5007 (2009).
- 702 53. Cavigelli, M., Dolfi, F., Claret, F. X. & Karin, M. Induction of c-fos expression through JNK-
703 mediated TCF/Elk-1 phosphorylation. *The EMBO Journal* **14**, 5957–5964 (1995).
- 704 54. Wood, C. D., Thornton, T. M., Sabio, G., Davis, R. A. & Rincon, M. Nuclear Localization of
705 p38 MAPK in Response to DNA Damage. *Int. J. Biol. Sci.* 428–437 (2009)
706 doi:10.7150/ijbs.5.428.
- 707 55. Tullai, J. W. *et al.* Immediate-Early and Delayed Primary Response Genes Are Distinct in
708 Function and Genomic Architecture. *J. Biol. Chem.* **282**, 23981–23995 (2007).
- 709 56. Fowler, T., Sen, R. & Roy, A. L. Regulation of Primary Response Genes. *Molecular Cell*
710 **44**, 348–360 (2011).
- 711 57. O’Donnell, A., Odrowaz, Z. A. & Sharrocks, A. D. Immediate-early gene activation by the
712 MAPK pathways: what do and don’t we know? *Biochemical Society transactions* **40**, 58–
713 66 (2012).
- 714 58. Ramirez-Carrozzi, V. R. *et al.* Selective and antagonistic functions of SWI/SNF and Mi-2 β
715 nucleosome remodeling complexes during an inflammatory response. *Genes Dev.* **20**,
716 282–296 (2006).
- 717 59. Goldstein, A. L. & McCusker, J. H. Three new dominant drug resistance cassettes for gene
718 disruption in *Saccharomyces cerevisiae*. *Yeast* **15**, 1541–1553 (1999).
- 719 60. Sheff, M. A. & Thorn, K. S. Optimized cassettes for fluorescent protein tagging in
720 *Saccharomyces cerevisiae*. *Yeast* **21**, 661–670 (2004).
- 721 61. Wosika, V. *et al.* New families of single integration vectors and gene tagging plasmids for
722 genetic manipulations in budding yeast. *Molecular Genetics and Genomics* **291**, 2231–
723 2240 (2016).
- 724 62. Chee, M. K. & Haase, S. B. New and Redesigned pRS Plasmid Shuttle Vectors for Genetic
725 Manipulation of *Saccharomyces cerevisiae*. *G3 (Bethesda)* **2**, 515–526 (2012).
- 726 63. Laughery, M. F. *et al.* New vectors for simple and streamlined CRISPR-Cas9 genome
727 editing in *Saccharomyces cerevisiae*. *Yeast* **32**, 711–720 (2015).
- 728 64. Pelet, S., Aymoz, D. & Durandau, E. Temporal quantification of MAPK induced expression
729 in single yeast cells. *J Vis Exp* (2013) doi:10.3791/50637.
- 730 65. Edelstein, A., Amodaj, N., Hoover, K., Vale, R. & Stuurman, N. Computer control of
731 microscopes using μ Manager. *Curr Protoc Mol Biol* **Chapter 14**, Unit14.20 (2010).
- 732 66. Unger, M., Lee, S.-S., Peter, M. & Koepl, H. Pulse Width Modulation of Liquid Flows:
733 Towards Dynamic Control of Cell Microenvironments. in *15th International Conference on*

734 *miniaturized systems for chemistry and life sciences : Microtas 2011* 1567–1569 (Chemical
735 and Biological Microsystems Society, 2011).
736 67. Unger, M. P. Interrogating the single cell: computational and experimental methods for
737 optimal live cell experiments. (ETH Zurich, 2014). doi:10.3929/ethz-a-010350761.
738

739 **End Notes**

740 *Acknowledgment*

741 We thank members the Pelet lab and Martin lab and for helpful discussions. Marta
742 Schmitt, Yves Dusserre, Gaëlle Spack, Joan Jordan and Clémence Varidel for
743 technical assistance. David Shore and his lab for helpful discussions and reagents.
744 Marie-Pierre Peli-Gulli and Claudio de Virgilio for plasmids, Tineke Lenstra for
745 suggesting the PP7 Δ FG allele. Agathe Pelet for manual curation of microscopy
746 images. Eulalia de Nadal, Mariona Nadal-Ribelles and Veneta Gerganova for critically
747 reading the manuscript. Work in the Pelet lab is supported by SystemsX.ch (IPhD
748 51PHP0_157354), the Swiss National Science Foundation (SNSF, PP00P3_172900
749 and 31003A_182431) and the University of Lausanne.

750 *Author Contributions*

751 VW and SP designed the experiments, analyzed the data and wrote the manuscript.
752 VW established the condition for the PP7 imaging. VW and SP performed the
753 experiments.

754 *Declaration of Interests*

755 The authors declare no competing interests.

756

757 **Figure Legends**

758 **Fig. 1. Monitoring the dynamics of osmostress-genes transcription.**

759 **a.** Schematics of the transcriptional response induced by the MAPK Hog1 upon
760 osmotic stress. Under normal growth conditions, the genomic locus is repressed by
761 histones set in place by the Ino80 complex and Asf1/Rtt109. In addition, H3K4
762 methylated histones mediated by Set1 contribute to the further repression of the locus

763 (upper panel). When Hog1 is active (lower panel), it accumulates in the nucleus with
764 the transcription factors Msn2/4. Hog1 binds to the transcription factors Hot1 and Sko1,
765 allowing the remodeling of the chromatin by Rpd3 and the SAGA complex. The
766 polymerases can be recruited to the locus and the RSC and SWR complexes evict
767 nucleosomes on the ORF. **b.** Construction of the transcriptional reporter. The promoter
768 of interest (*pPROM*) is cloned in front of 24 stem-loops (*24xPP7sl*). This construct is
769 transformed in yeast and integrated in the *GLT1* locus 5'UTR, replacing the
770 endogenous promoter. Upon induction of the promoter, the mRNA stem-loops are
771 transcribed and recognized by the fluorescently-tagged PP7 phage coat protein. **c.**
772 Maximum intensity projections of Z-stacks of microscopy images from the *pSTL1-*
773 *PP7sl* reporter system in a 0.2M NaCl osmotic stress time-lapse experiment. The
774 appearance of bright foci (arrow heads) in the nucleus of the cells denotes the active
775 transcription arising from the promoter. Scale bar represents 5 μm . **d.** Dynamics of the
776 *pSTL1-PP7sl* transcription site intensity (20 brightest pixels in the nucleus minus the
777 median fluorescence of the cell) following hyperosmotic stress. The mean from 200 to
778 400 cells is represented by the solid line. The shaded areas represent the s.e.m. **e.**
779 Analysis of one representative single-cell trace. The raw trace (gray) is smoothed with
780 a moving average (dark blue) and normalized by subtracting the intensity of the first
781 time point after the stimulus. Multiple quantitative values can be extracted from this
782 trace (see Methods). Source data are provided for d.

783

784 **Fig. 2. Chromatin state dictates the transcription initiation of stress-induced**
785 **promoters**

786 **a.** Dynamics of the transcription site intensity from six different promoters following a
787 0.2M NaCl stress. The mean of at least 140 cells is represented by the solid line. The
788 shaded areas represent the s.e.m. **b.** Percentage of cells where a PP7 TS site was
789 detected. The light shaded area represents the percentage of PP7 positive cells before
790 the stimulus was added (basal transcription). **c.** The microscopy thumbnails display
791 cells bearing the *pGPD1-PP7sl* reporter system, where transcription sites (arrow
792 heads) can be detected before and after the stress of 0.2M NaCl. Scale bar represents
793 5 μm . **d.** Cumulative distribution function (CDF) of the Start Time for each promoter

794 considering only the cells that induce transcription after time zero. **e.** 10th, 50th and 90th
795 percentiles of the Start Times shown for the two to three replicates measured for each
796 promoter. The number of stars next to each measurement corresponds to the number
797 of promoters without basal level that are significantly different from the promoter with
798 basal level (two-sample *t*-test, $p < 0.05$). **f.** Cumulative distribution functions of Start
799 Times for the p*STL1*-PP7sl strain in wild type, *htz1Δ* or *gcn5Δ* backgrounds. The inset
800 shows the percentage of PP7 positive cells in each background. **g.** Cumulative
801 distribution functions of Start Times for the p*STL1*-PP7sl strain grown in glucose or
802 raffinose. The inset shows the percentage of PP7 positive cells, the light blue bar the
803 basal positive PP7 cells. Source data are provided for a, f, g.

804

805 **Fig. 3. Early Hog1 activity dictates promoter activation and output**

806 **a.** In Hog1 nuclear relocation traces obtained from single cells, the timing of Hog1
807 nuclear entry (■), maximum enrichment (●), start of the decay in nuclear enrichment
808 (◆) and Hog1 adaptation (▲) can be identified (upper panel). The median (marker)
809 and 25th to 75th percentiles (lines) for these measurements are plotted for three
810 different osmotic stresses (central panel). The cumulative distribution functions of Start
811 Times for the p*STL1*-PP7sl reporter for these same three concentrations are plotted
812 (lower panel). **b.** Histograms of Start Times following a 0.2M stress for the five other
813 promoters tested. The vertical dashed line represents the median decay time of Hog1
814 measured at 0.2M. The number in the legend indicates the percentage of cells which
815 have initiated transcription before the median Hog1 decay time. **c.** The population of
816 p*STL1*-PP7sl positive cells is split in four quartiles based on their Start Time. The
817 median (●) and 25th to 75th percentiles (line) of the integral of the PP7 trace is plotted
818 for each quartile. Source data are provided for a.

819

820 **Fig. 4. Transcription factors control the dynamics and level of mRNA production**

821 **a.** Violin plots of the trace intensity (maximum of the TS during the transcription period)
822 for the six promoters after stimulation by 0.2M NaCl. Each dot represents the value
823 calculated from a single cell. The solid line is the median and the dashed line the mean

824 of the population. **b.** Comparison between the trace intensity in stimulated (0.2M NaCl)
825 and unstimulated conditions (0.0M) for the three promoters displaying basal
826 expression. **c. - f.** Effect of the deletions of the *HOT1* and *SKO1* transcription factor
827 genes on p*STL1* and p*GPD1* dynamics of transcription (c), cumulative distribution
828 functions of Start Times (d), the trace intensity (e) and the percentage of responding
829 cells (f) for the p*STL1*-PP7sl and p*GPD1*-PP7sl reporter strains following a 0.2M NaCl
830 stress for at least 200 cells. For the p*STL1*-PP7sl *hot1* Δ sample, 349 cells were
831 analyzed with only 9 displaying a PP7 positive signal. This low number does not allow
832 to draw a meaningful CDF curve in panel d. Source data are provided for b and c.

833

834 **Fig. 5. Identification of transcription bursts in stress-induced transcription.**

835 **a.** Percentage of cells where 1, 2 and 3 or more peaks are identified among the
836 population of responding cells for the different promoters following a 0.2M NaCl stress.
837 **b.** Examples of single-cell traces displaying 1 or 2 peaks for the p*STL1*-PP7sl and the
838 p*GPD1*-PP7sl reporter strains. **c.** Violin plots representing the Peak Duration. Each dot
839 represents the value calculated for a single peak. The solid line is the median and the
840 dashed line the mean of all the peaks measured. **d. - e.** The population of cells was
841 split between cells displaying one peak and two or more peaks. The Peak Duration (d)
842 and Trace Intensity (e) are plotted for the p*HSP12*-PP7sl and p*GPD1*-PP7sl strains.
843 Each dot represents the value calculated for a single peak (d) or a single cell (e). The
844 solid line is the median and the dashed line the mean of the population.

845

846 **Fig. 6. Hog1 activity and promoter identity control the shutoff of transcription**

847 **a.** Violin plots representing the Transcription Period (time difference between End Time
848 and Start Time) measured for the p*STL1*-PP7sl reporter following 0.1, 0.2 and 0.3M
849 NaCl stresses. Each dot represents the value calculated from a single cell. The solid
850 line is the median and the dashed line the mean of the population. **b.** One minus the
851 cumulative distribution function of End Times for the p*STL1*-PP7sl reporter. The
852 vertical dashed lines represent the median adaptation time of Hog1 for the three
853 different stress levels. **c.** Dynamics of the estimated NaCl concentrations in the
854 medium for the pulse, step and ramp experiment protocols (upper panel, Methods).

855 Corresponding Hog1 relocation dynamics (middle panel) and pSTL1-PP7sl
856 transcription site intensity (lower panel). The mean of at least 180 cells is represented
857 by the solid line. The shaded areas represent the s.e.m. **d.** Cumulative distribution
858 function (CDF) of the Start Time for all cells in the pulse, step and ramp experiments.
859 The CDF at 15 min represents the fraction of responding cells for each condition. **e.**
860 One minus the cumulative distribution function of End Times only for the responding
861 cells in the pulse, step and ramp experiments. **f.** Correlation between the Hog1
862 adaptation time and the PP7 End Time measured in the same cells in the pulse, step
863 and ramp experiments. The open markers indicate cells where Hog1 has not adapted
864 at the end of the time lapse. Adaptation time is arbitrarily set to 35 min for this sub-
865 population. Source data are provided for c.

866

867 **Fig. 7. Transcription shutoff from different promoters**

868 **a.** Violin plots representing the Transcription Period measured for the six different
869 promoters following a 0.2 NaCl stress. Each dot represents the value calculated from
870 a single cell. The solid line is the median and the dashed line the mean of the
871 population. **b.** One minus the cumulative distribution function of End Times for the
872 different promoters. The vertical dashed line represents the median adaptation time of
873 Hog1 at 0.2M NaCl.

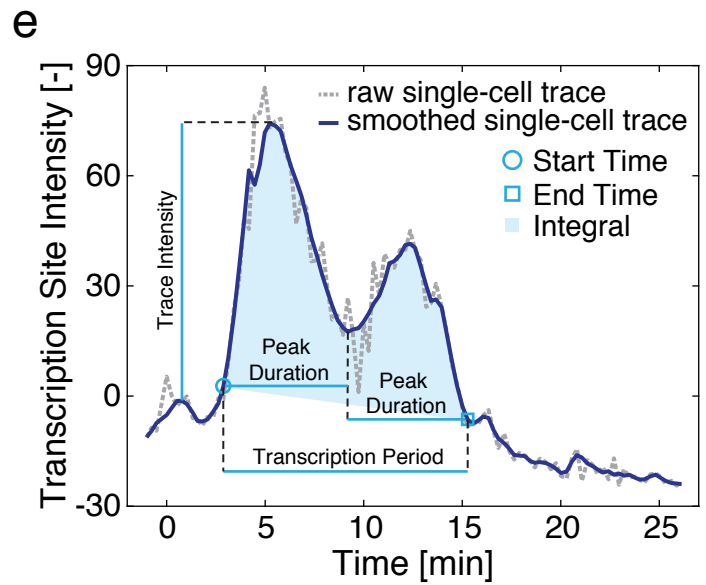
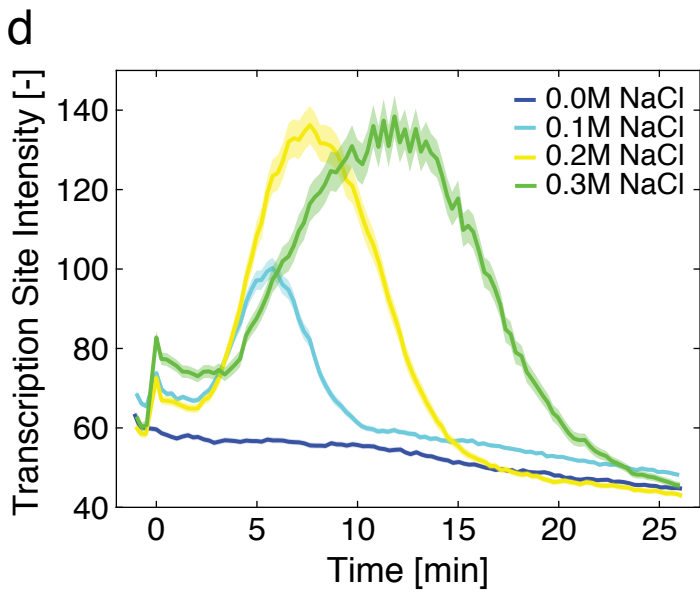
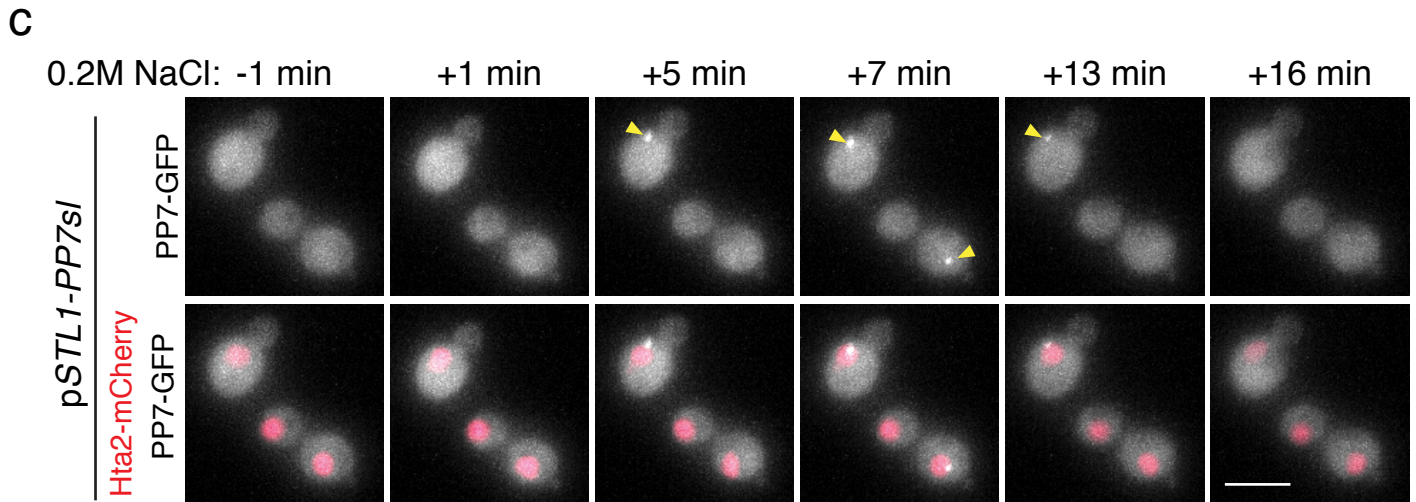
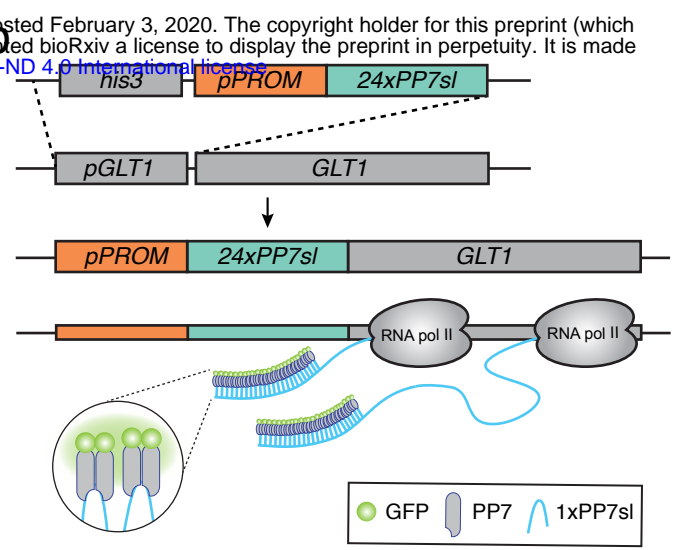
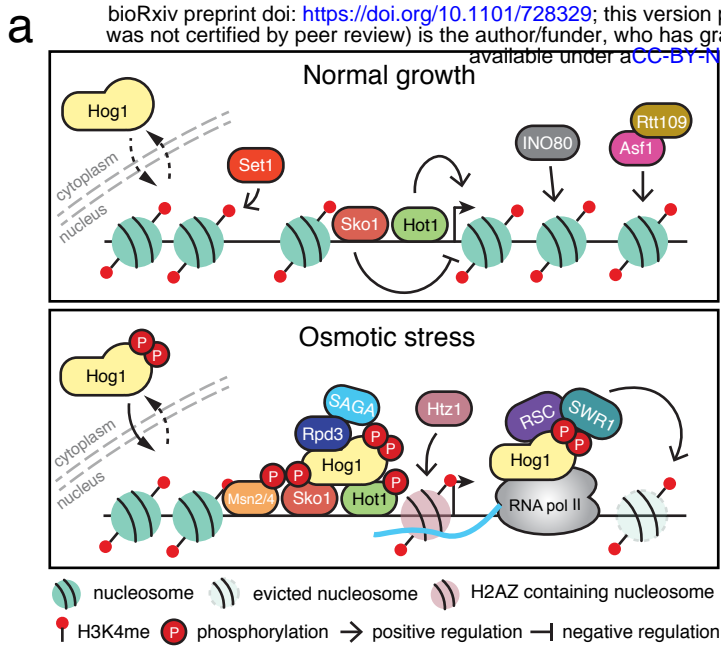


Figure 1

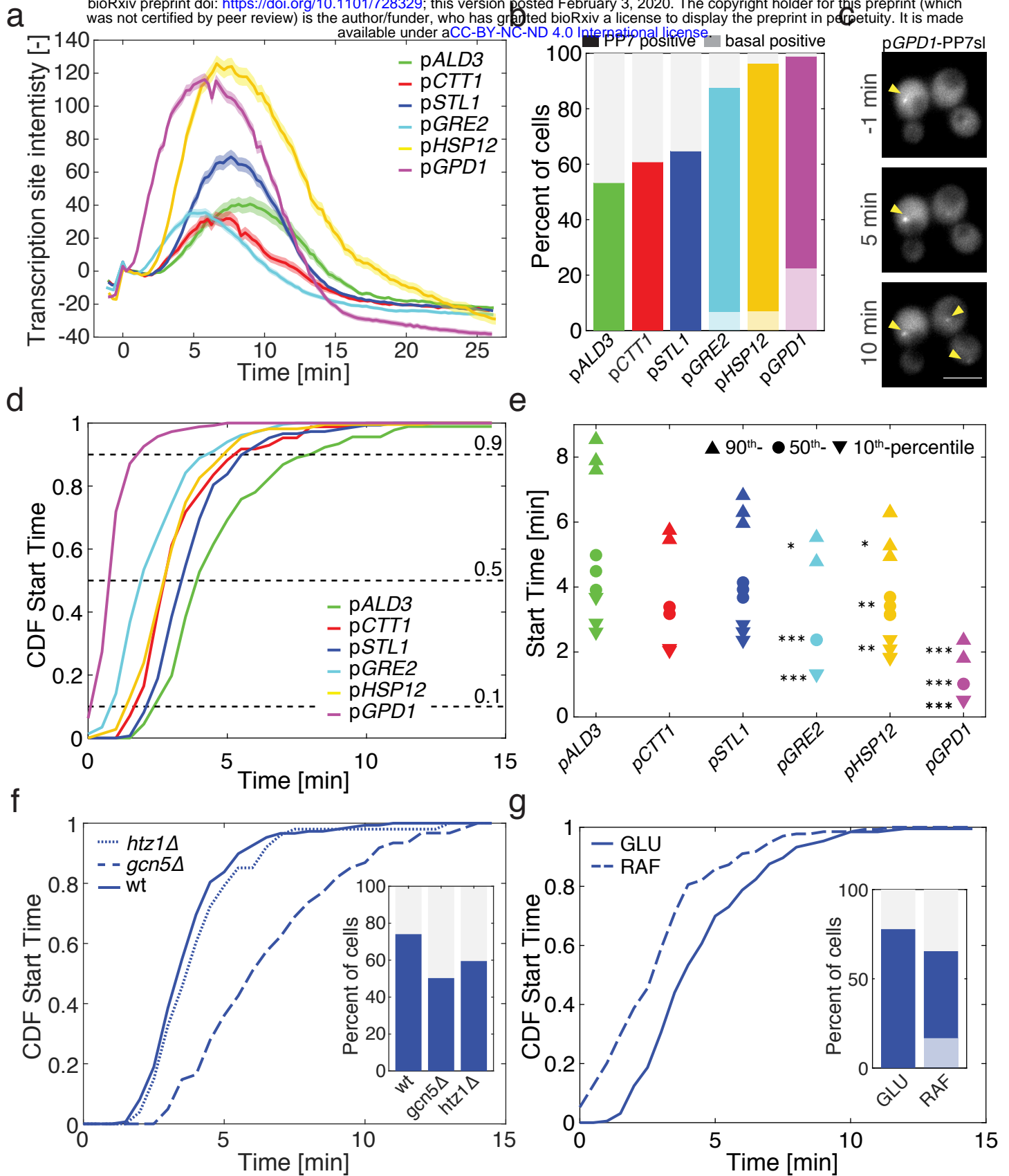


Figure 2

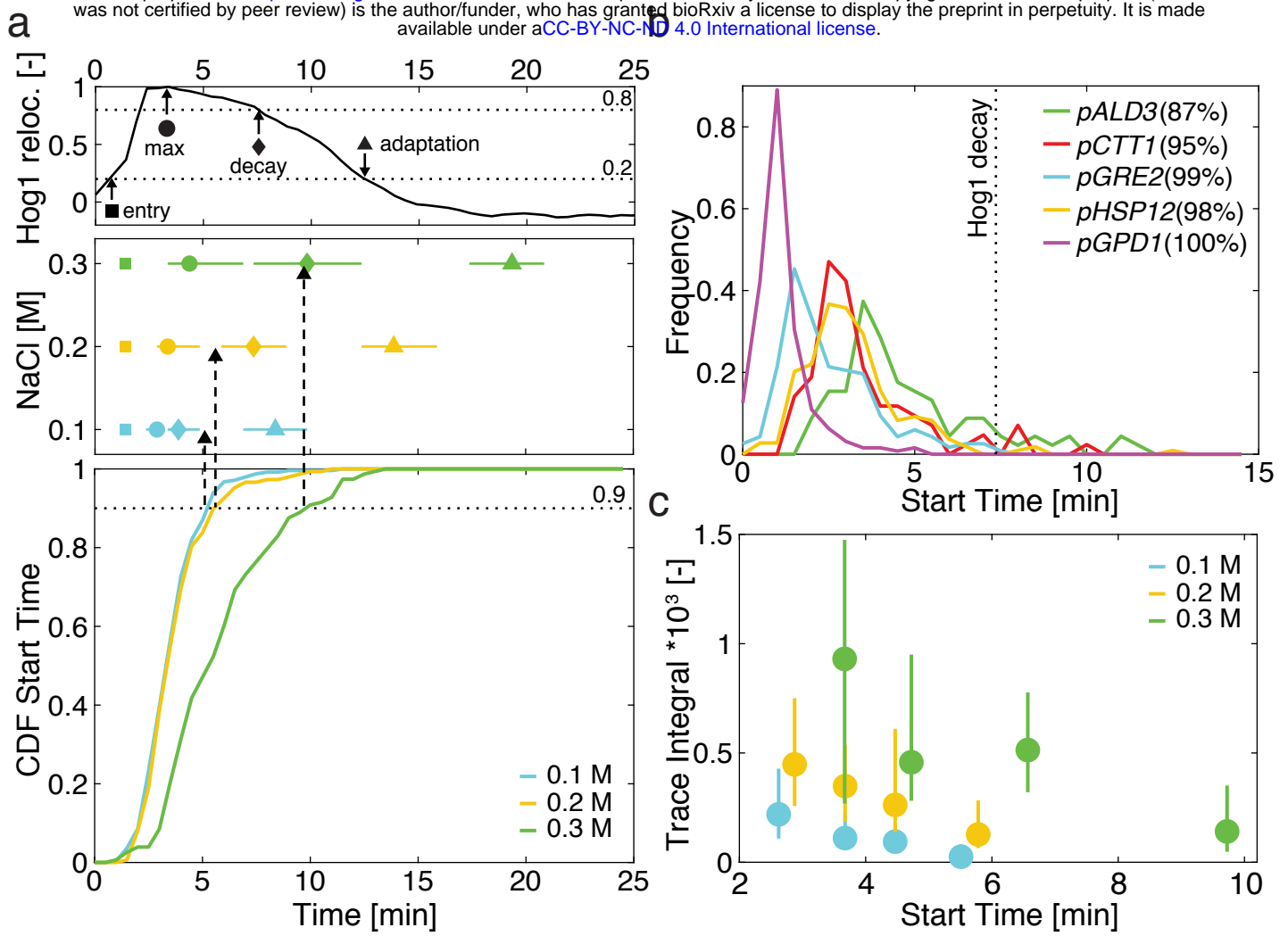


Figure 3

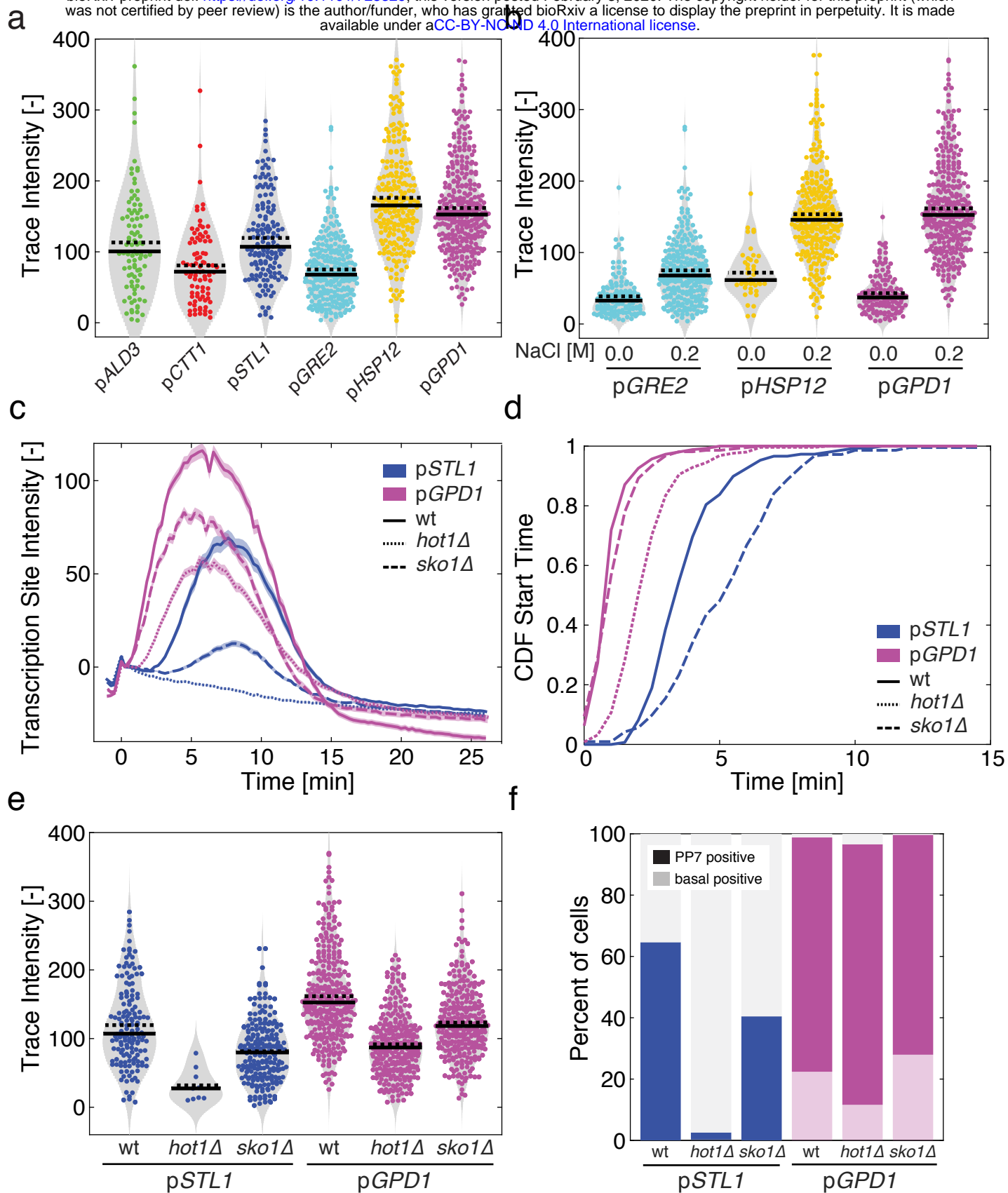


Figure 4

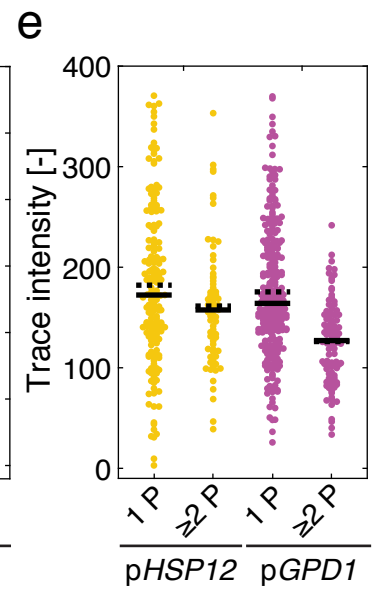
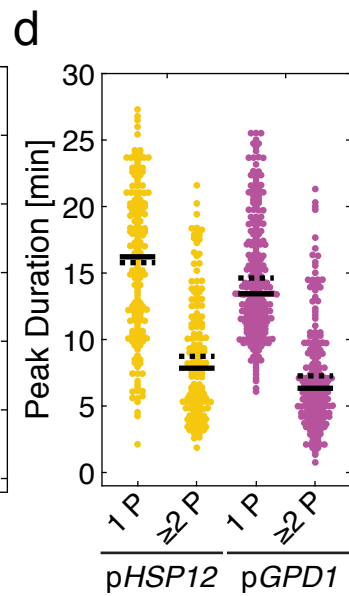
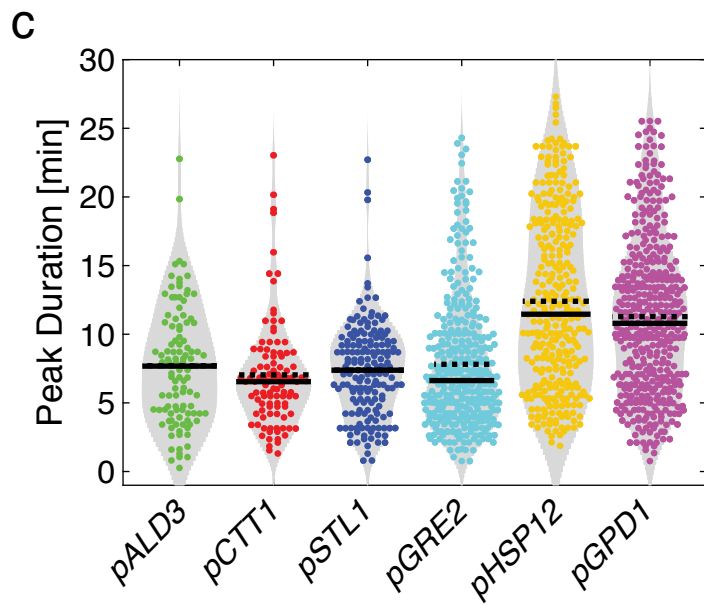
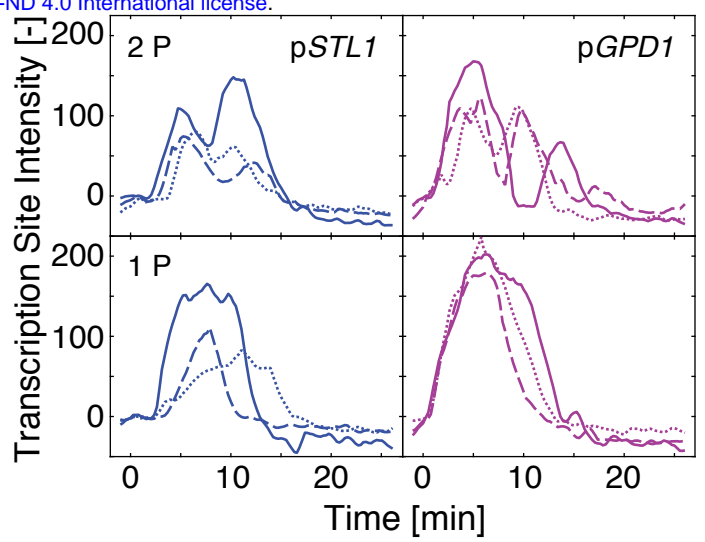
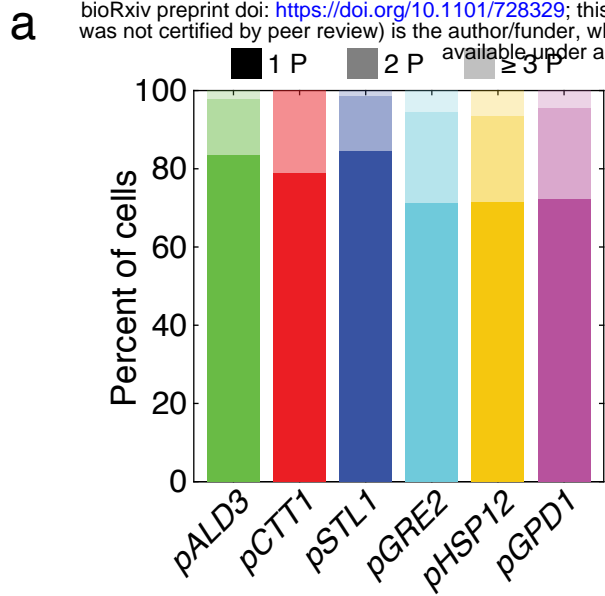


Figure 5

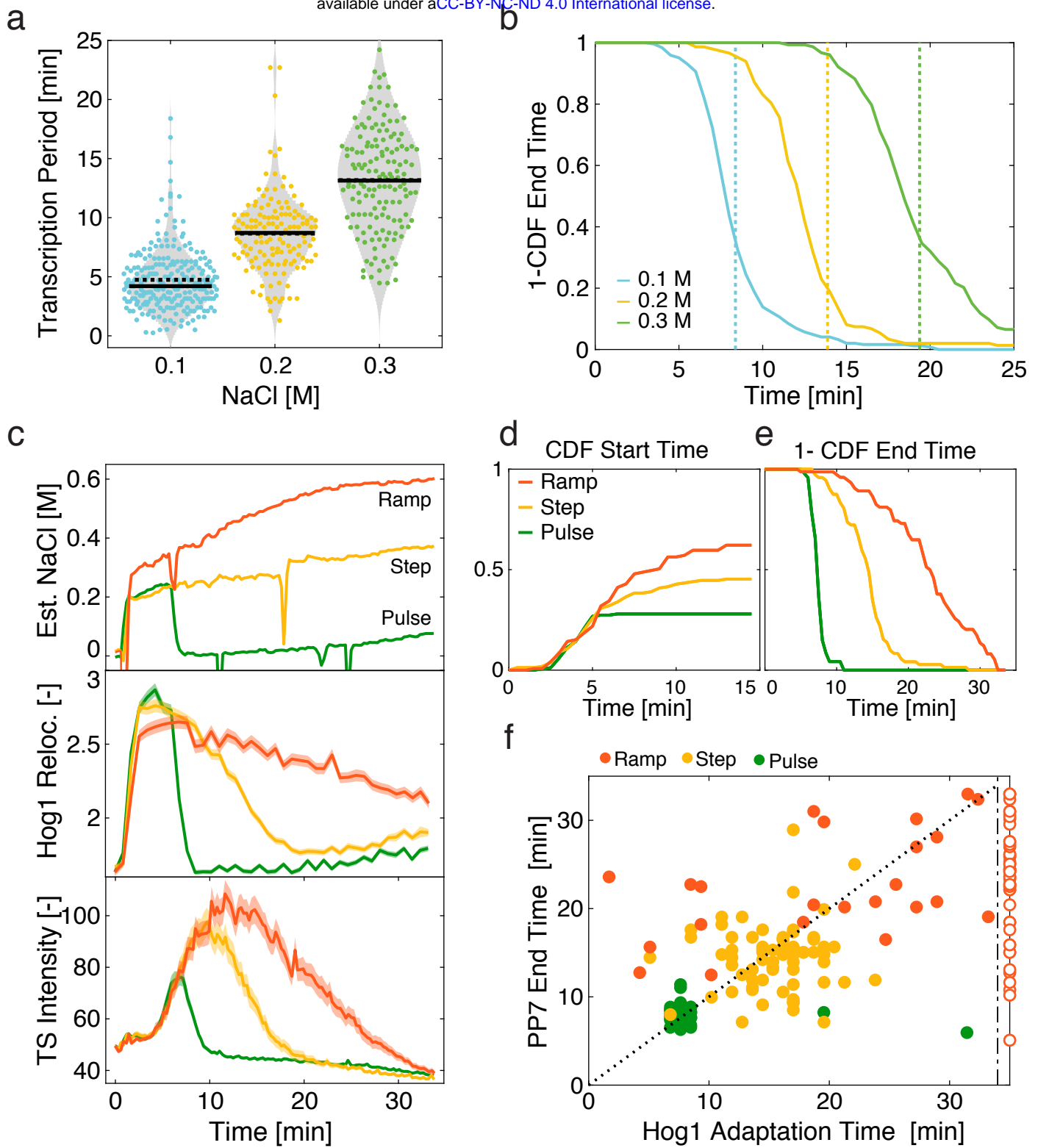


Figure 6

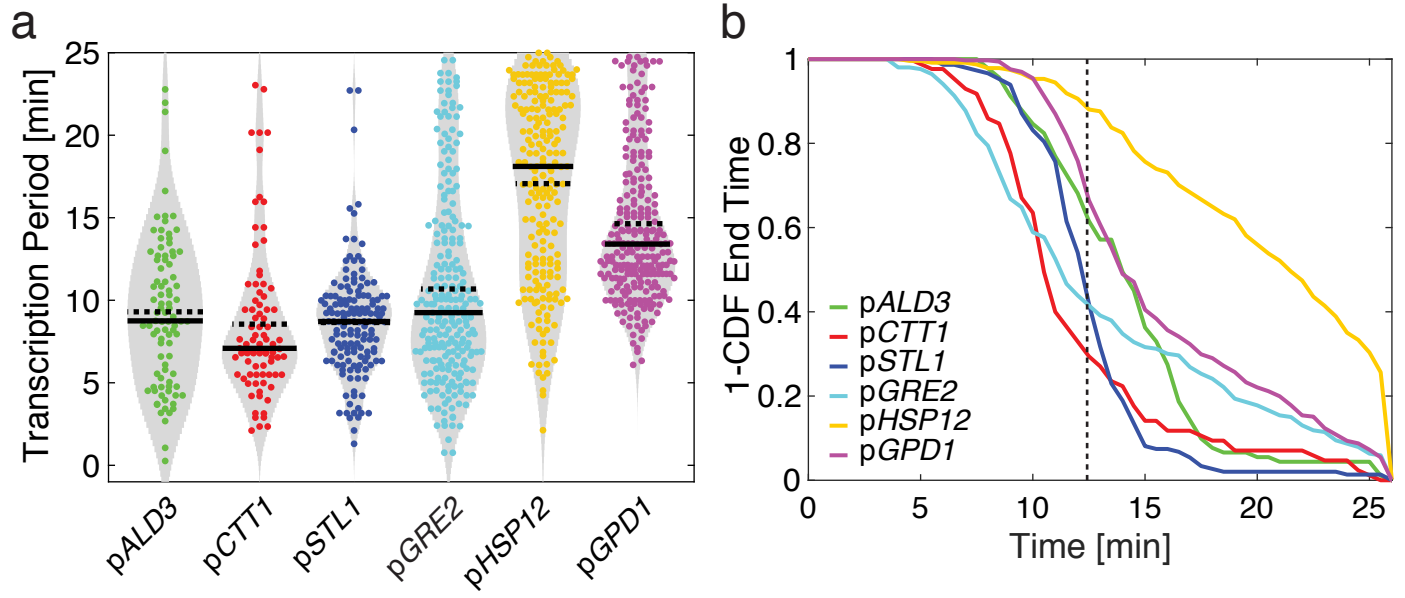


Figure 7